nature climate change

LETTERS

https://doi.org/10.1038/s41558-019-0648-9

Phenology of nocturnal avian migration has shifted at the continental scale

Kyle G. Horton[1*], Frank A. La Sorte[2], Daniel Sheldon[3,4], Tsung-Yu Lin[3], Kevin Winner[3], Garrett Bernstein[3], Subhransu Maji[3], Wesley M. Hochachka[2] and Andrew Farnsworth[2]

Climate change induced phenological shifts in primary productivity result in trophic mismatches for many organisms[1–4], with broad implications for ecosystem structure and function. For birds that have a synchronized timing of migration with resource availability, the likelihood that trophic mismatches may generate a phenological response in migration timing increases with climate change[5]. Despite the importance of a holistic understanding of such systems at large spatial and temporal scales, particularly given a rapidly changing climate, analyses are few, primarily because of limitations in the access to appropriate data. Here we use 24 years of remotely sensed data collected by weather surveillance radar to quantify the response of a nocturnal avian migration system within the contiguous United States to changes in temperature. The average peak migration timing advanced in spring and autumn, and these changes were generally more rapid at higher latitudes. During spring and autumn, warmer seasons were predictive of earlier peak migration dates. Decadal changes in surface temperatures predicted spring changes in migratory timing, with greater warming related to earlier arrivals. This study represents one of the first system-wide examinations during two seasons and comprises measures from hundreds of species that describe migratory timing across a continent. Our findings provide evidence of spatially dynamic phenological shifts that result from climate change.

Scale is a fundamental consideration in assessing the magnitude of climate change impacts, whether spatial, temporal or taxonomic. Broad perspectives are required to understand how climate change affects entire systems. Organisms are now displaying a number of ecological and evolutionary responses to climate change[6], which include shifts in their phenologies. As climate change leads to shifts in the phenology of primary productivity[7], mismatches are occurring at higher trophic levels. Seasonal migration represents a system for which broader perspectives would be invaluable. For example, with migratory birds, the peak demand for insect prey may occur after the peak supply, which results in a mismatch of resources[8,9]. For migratory birds that use many ecosystems at a diversity of scales, changes in phenology may directly impact the population distributions and ultimately lead to expansion or extirpation[2,10].

Numerous mechanisms for phenological shifts and mismatches exist[4,8,11]. Migratory birds synchronize movements in time and space with seasonal food resources, which magnifies risks of dramatic mismatches and the effects thereof. For birds that migrate long distances to winter in the tropics, endogenous cues together with subtle but predictable exogenous cues, such as photoperiod, entrain migratory departure behaviours[12]. However, these cues may conflict with highly variable exogenous cues encountered en route. As a result, populations that travel long distances in the spring may be slow to adapt the timing of departure and other migratory behaviours to rapid climatic changes that occur elsewhere[13]. Conversely, populations that travel shorter distances may experience closer relationships between exogenous cues that initiate movements and cues representing important phenological shifts en route[14]. Species that do not shift their phenologies may exhibit population declines, assuming they do not increase fitness in other portions of their annual cycle, whereas those that adjust their migration timing may maintain or increase population size[15].

We do not understand how individual-level changes in migration phenology scale to affect an entire migration system[16,17]. To date, challenges in measuring phenology at scales that capture the full extent of migratory events have constrained inferences. Phenological change can be incremental, and often requires long time series to detect shifts. Changes in climate are spatially variable and observations across broad spatial extents are essential to capture differential responses. Much of our knowledge about avian responses to climate change originates from individual-based studies[4,18,19]. Inferences that originate from individual-level studies can be constrained and open to biological and statistical biases based on the species under consideration and where and when they were sampled. A broader view of avian responses that represents diverse assemblages of migrants, captures continental movements at an aggregate level and samples across long time periods during spring and autumn migration would provide a unique insight into phenological changes driven by changing climate[16].

Advances in remote-sensing technologies have enhanced our ability to quantify phenological changes. These platforms provide repeated and consistent observations over time. Most notably, they have led to the development of large-scale vegetation indices[20]. Remote-sensing platforms for animals are rarer, but the US weather surveillance radar (WSR) network is emerging as a comprehensive source of information about flying animals. Radars have revealed numerous insights into avian migration[21], but only recent advances in data access and processing allow the examination of weather radar archives to study long-term phenological change[22]. The use of WSRs avoids many of the sampling biases associated with individual-based examinations by providing a comprehensive representation of the entire migration signal across the full migration season and across a considerable portion of the longitudinal breadth of the migration system. The methods employed in this study can be readily replicated annually, which allows for the long-term

[1]Department of Fish, Wildlife, and Conservation Biology, Colorado State University, Fort Collins, CO, USA. [2]Cornell Lab of Ornithology, Cornell University, Ithaca, NY, USA. [3]College of Information and Computer Sciences, University of Massachusetts, Amherst, MA, USA. [4]Department of Computer Science, Mount Holyoke College, South Hadley, MA, USA. *e-mail: kyle.horton@colostate.edu

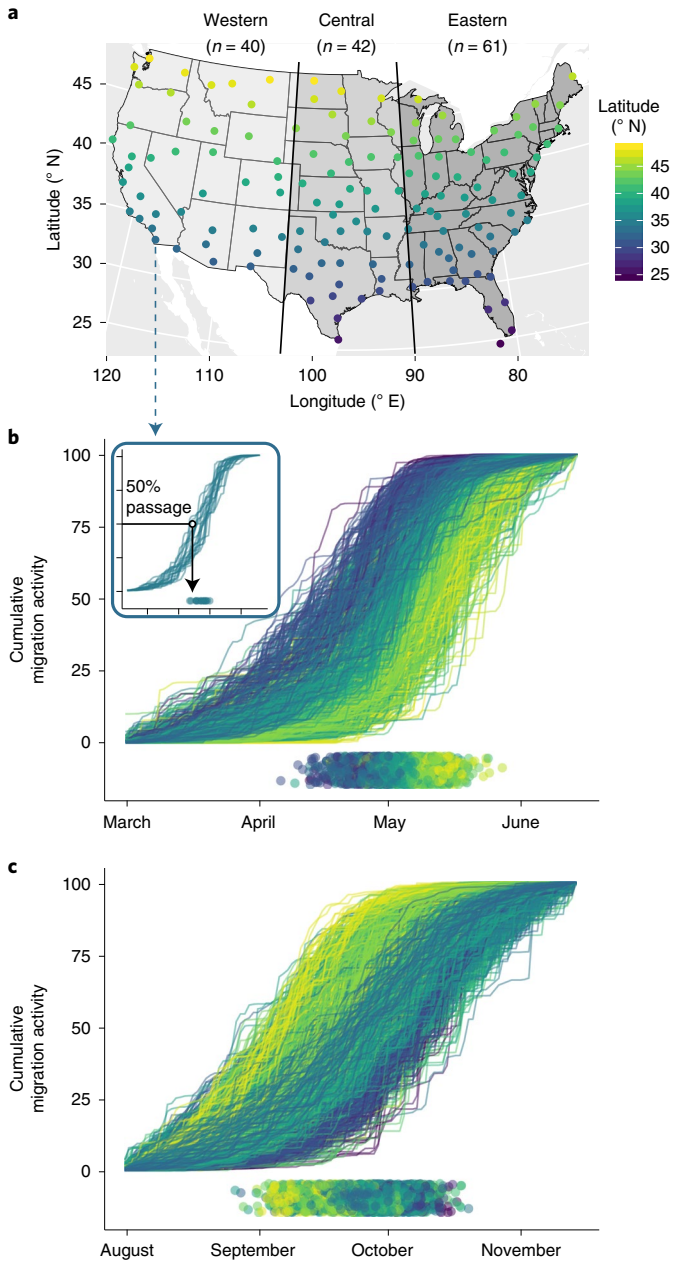

Fig. 1 | WSR locations and phenological time series. a, WSR stations and corresponding migratory flyways. **b**,**c**, Yearly cumulative migration activity for 143 WSR stations for spring and autumn from 1995 to 2018. Peak migration dates (that is, date at which 50% of cumulative activity occurred) are shown as circles below each curve. Station locations, cumulative lines and dates of 50% passage are shaded according to station latitude. Latitude predicted the date of peak migration for both seasons (linear mixed-effect model with year as the random effect, spring $P<0.001$, autumn $P<0.001$). Spring migration showed a more rapid pace across latitude (spring, 0.83 ± 0.04 d per degree of latitude; autumn, -0.68 ± 0.06 d per degree of latitude).

monitoring of migration phenology in a consistent and rigorous fashion. To this end, we examined the past 24 years of radar data collected over the continental United States to study the phenology of nocturnally migrating birds. We provide the first system-based indices of migration phenology and test whether migration timing has shifted at these large scales. We focus on peak migration, defined as the date by which 50% of the cumulative passage occurred, to examine the timing of migration through the biogeographically distinct western, central and eastern flyways[23] across 143 radar sampling locations (Fig. 1). We predicted that peak migration dates would advance with warming seasonal temperatures and changes would be greatest at northern latitudes where the magnitude of warming is strongest[24,25].

We sampled 2,115 spring nights and 2,152 autumn nights, with a total of over 13 million radar scans from 1995 to 2018. To test whether migration timing changed, we used a generalized-additive mixed model to examine change in the peak migration date across years and latitude (Fig. 2). The peak spring migration generally advanced, and more so with increasing latitude (Fig. 2a). Considerable advances in spring timing occurred at 35, 40 and 45° N; however, no change was apparent at 30° N (Fig. 2b). Examining the decadal trends in peak migration date at individual WSR stations, using least-squares linear regression, the mean change was similar across all three flyways (Fig. 3a) (analysis of variance: $F_{2,140}=2.717$, $P=0.0695$), with a mean advancement of 0.60 ± 0.15 d decade^{-1} (throughout the article, $\pm$ refers to the 95% confidence interval).

The autumn phenological changes were similar to those that occurred in spring (that is, an earlier peak migration), although the changes were weaker, especially at northern latitudes (Fig. 2c). At 40 and 45° N, the magnitude of advance in the autumn was approximately half that in the spring (Fig. 2d). The western flyway showed the strongest advances (-0.89 ± 0.14; Fig. 3b) and a significantly different coefficient of change (Tukey honestly significant difference, $P<0.001$) as compared to the much weaker eastern (-0.52 ± 0.12; Fig. 3b) and central (-0.34 ± 0.18; Fig. 3b) flyway trends.

Spring air temperatures at 2 m above ground level increased over this same time period (mean 0.58 ± 0.06 °C decade^{-1}; Fig. 3c), with the greatest changes occurring within the central flyway (0.72 ± 0.06 °C decade^{-1}). Temperature changes differed significantly across flyways (Tukey honestly significant difference, $P<0.001$), except between western and eastern regions ($P=0.85$). Within the radar coverage areas, the rate of change of average spring temperature varied between −0.36 and 1.49 °C decade^{-1}, with 96% of the stations (137 of 143 stations) showing a warming trend (Fig. 3c). Similarly, the autumn period showed increasing air temperatures (mean 0.54 ± 0.05 °C decade^{-1}; Fig. 3d); however, temperature changes did not differ significantly across flyways (analysis of variance: $F_{2,140}=0.87$, $P=0.421$). The autumn slopes varied between −0.03 and 1.32 °C decade^{-1}, with 94% of the stations (134 of 143 stations) showing a warming trend (Fig. 3d).

At the yearly timescale, we compared anomalies (deviations from station-specific means) in phenology to those in temperature using least-squares linear regression. We examined the 10th and 90th percentiles of passage date in addition to the peak (that is, median) to capture the earlier and later phases of migration. Spring temperature anomalies predicted median passage date anomalies (slope $=-0.74\pm0.10$, $F_{1,2694}=215.7$, $P<0.001$, $R^2=0.07$; Fig. 4a). Early spring passage-date anomalies (10th percentile) showed the steepest slope (slope $=-1.40\pm0.17$, $F_{1,2694}=251.9$, $P<0.001$, $R^2=0.09$; Fig. 4a) and late periods (90th percentile) showed the shallowest (slope $=-0.35\pm0.10$, $F_{1,2694}=45.24$, $P<0.001$, $R^2=0.02$; Fig. 4a). During all three autumn periods, the temperature anomalies predicted the median passage date anomalies, yet with weaker coefficients (10th percentile, slope $=-0.51\pm0.17$, $F_{1,2636}=34.17$, $P<0.001$, $R^2=0.01$; 50th percentile, slope $=-0.29\pm0.15$, $F_{1,2636}=13.8$, $P<0.001$, $R^2=0.01$; 90th percentile, slope $=-0.37\pm0.15$, $F_{1,2636}=23.94$, $P<0.001$, $R^2=0.01$; Fig. 4b).

At the decadal timescale, changes in seasonal temperature predicted spring phenological change within the western (slope $=-1.09\pm0.89$, $F_{1,38}=5.83$, $P<0.05$, $R^2=0.13$; Fig. 4b) and eastern (slope $=-0.91\pm0.61$, $F_{1,59}=8.60$, $P<0.01$, $R^2=0.13$; Fig. 4b) flyways, but not the central (slope $=-0.52\pm0.56$, $F_{1,40}=3.32$, $P=0.0759$, $R^2=0.08$; Fig. 4b)—although all the flyways' spring

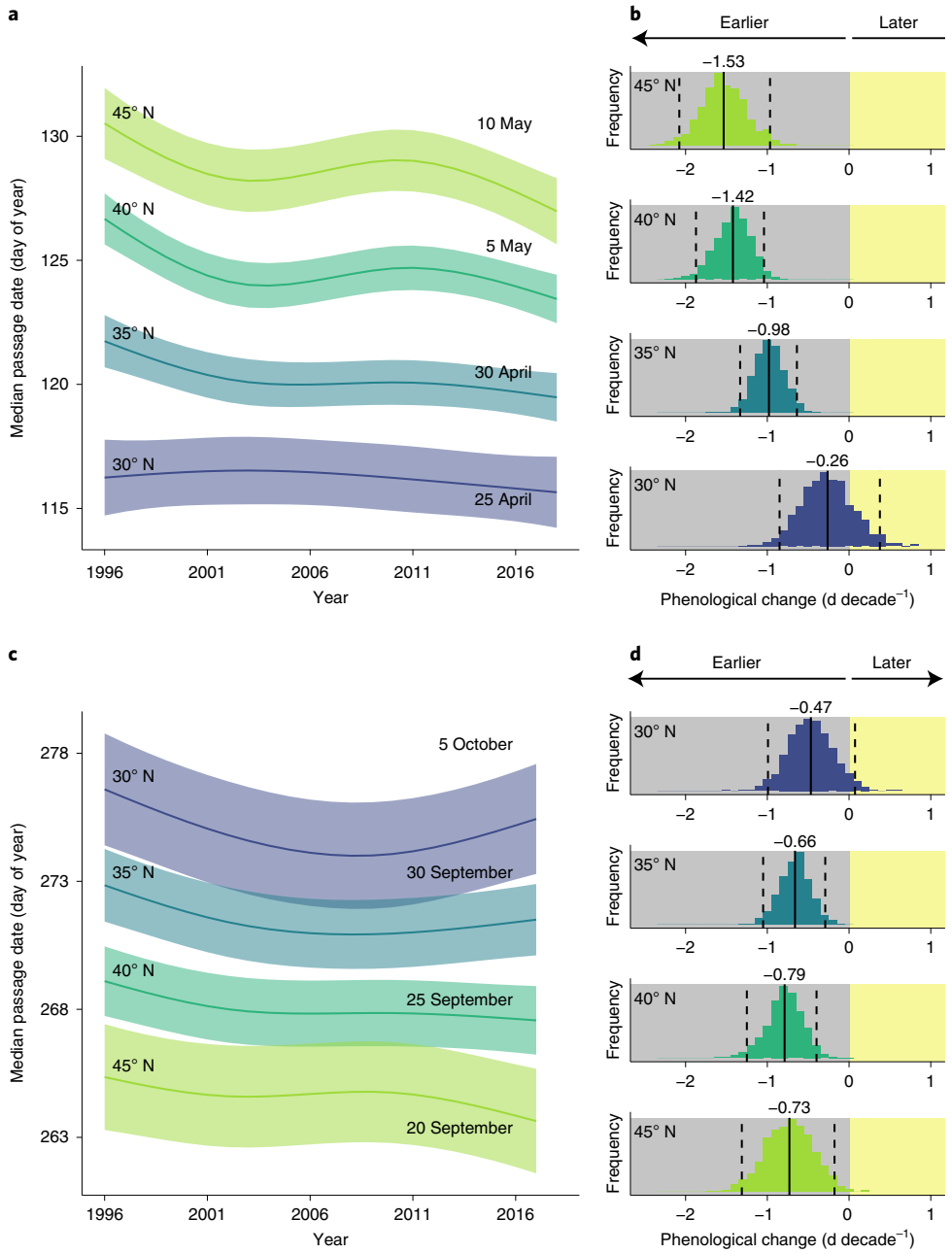

Fig. 2 | Predicted seasonal phenological change. a,**c**, Predicted peak spring (**a**) and autumn (**c**) migration dates by year at 143 WSR stations. The fitted lines and 95% confidence bands are derived from a generalized additive mixed model (GAMM). **b**,**d**, Distributions of phenological change extracted from 1,000 bootstrapped GAMM samples. The solid lines show the mean of the distribution and the dashed lines the 5th and 95th percentiles. The lines and histograms are shaded by latitude (colour scale as in Fig. 1). Note that the *y* axes of **b** and **d** represent frequency, each of which have a different maxima, but the same summed total number of samples (1,000).

relationships exhibited the same directional pattern (that is, positive slopes). Autumn relationships were not significant in the western (slope = −0.12 ± 0.87, $F_{1,38} = 0.07$, $P = 0.794$, $R^2 = 0.002$; Fig. 4d), central (slope = 0.76 ± 1.56, $F_{1,40} = 0.90$, $P = 0.347$, $R^2 = 0.02$; Fig. 4d) or eastern (slope = −0.36 ± 0.66, $F_{1,59} = 1.14$, $P = 0.291$, $R^2 = 0.02$; Fig. 4d) flyways.

Our system-level timing measurements arise from a diverse collection of migration strategies, which include long and short distances, and partial and full, obligate, facultative and irruptive movements. Despite this variation, significant changes in the timing of bird migration have occurred at the continental scale based on an aggregate measure of nocturnal migration using a network of standardized sensors (that is, WSR-88D). We observed shifts in timing of movements associated with an expected currency of climate change—temperature. In the spring, we saw the strongest association with annual temperature during the earliest periods (for example, 10th percentile), a period of time probably dominated by the shortest-distance migrants[21] and most flexible in their adjustments to resource availability. Observed increases in air temperature in the spring were predictive of changes in the migration timing, with a greater warming relating to earlier arrivals in the spring for all flyways. This is the first analysis of the entire 24-year WSR-88D archive in the contiguous United States. At these scales, changes comprise millions of migrating birds of hundreds of species. Numerous

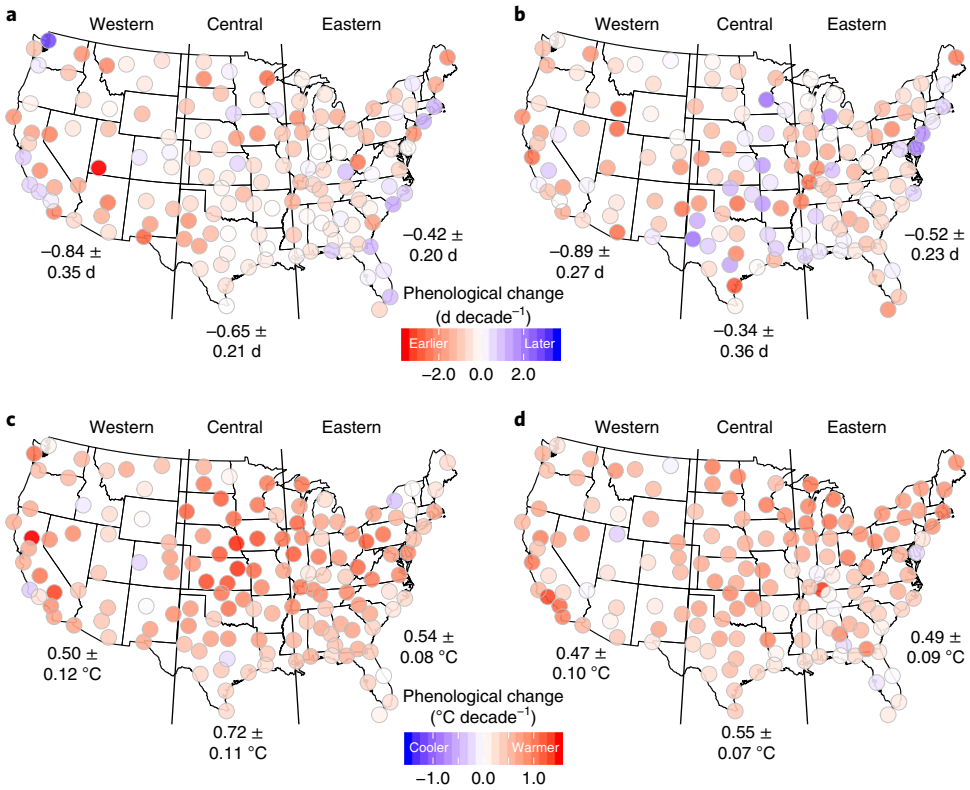

Fig. 3 | Change in spring and fall migration phenology and temperature across 143 WSR stations. a,**b**, Phenological change for spring (**a**) and autumn (**b**) at each WSR station. The mean phenological change and 95% confidence intervals are displayed below each flyway. **c**,**d**, Temperature change for spring (**c**) and autumn (**d**) at each WSR station. The mean temperature change and 95% confidence intervals are shown towards the bottom of each flyway.

studies hinted at the value of such an analysis[16,26], but it was previously impossible in the absence of a combination of advanced machine learning, data accessibility and interoperability.

The diverse and complex system of behaviours that compose birds' migration strategies have evolved in direct relation to changing climates[27]. Changing resource availabilities during periods of significant climatic change presumably influenced the ecological and evolutionary histories of many species, and that individuals and species respond to climate-driven changes in their environments is not surprising. Our results show a continental shift in migration timing, particularly during spring, but the rate of change at this scale is limited (for example, about <2 d decade^{-1}), and may not match the rapidity of climate-induced shifts in resource availability[17]. Autumn patterns of decadal phenological change were variable and not predicted by changing temperatures, but warmer years generally resulted in earlier median passage dates (Fig. 4c)[28]. Additional sources of variation in autumn, which included a relaxed arrival pressure and variable departure dates stratified by age, sex and success of breeding[29] probably result in more muted aggregate responses to changing climates.

Numerous factors may be responsible for the variation in our results among seasons, flyways and latitude. We observed stronger phenological changes at higher latitudes, especially during spring, which highlights the need for large-scale analyses of phenological change: spatial gradients can result in highly variable conclusions of phenological change. It is unclear whether this latitudinal trend represents differential responses across populations and species, and/or whether phenological plasticity at the level of the individual is responsible. Whereas fixed exogenous cues (for example, photoperiod) probably trigger the spring departure from wintering grounds[12]—which results in relatively consistent arrival dates at southern latitudes (Fig. 2a)—behavioural changes en route may allow migrants to recalibrate their pace based on proximate resource availability. If so, what mechanism is responsible for this change in pace? Reducing stopover duration has the capacity to allow migrants to track resource availability[30,31], but the degree of achievable change by this mechanism may be limited for some species (that is, stopover is essential) and may not match sustained shifts in resource availability without matching shifts in the initiation of migration.

Regardless of the underlying mechanisms, our findings highlight geographical differences in migration systems of the continental United States. We observed the most rapid rates of change in the western flyway, the part of the continental migration system with the largest number of species migrating the shortest distances[23] and perhaps most apt to exhibit systemic responses to changing resource availability. However, the western flyway is also notably understudied[32] and is characterized by complex weather, atmospheric and topographical features, all of which presumably drive phenological patterns.

The integration of additional information on species-specific patterns, for example, from citizen science or individual tracking, is a priority to clarify specific mechanisms of phenology change[30,31,33]. Acquiring sufficient time-series data from these sources of information is challenging, but increasingly possible. Furthermore, a greater understanding of the spatial resolution of phenological change is important, as the macroclimate and microclimate may interact within regions for numerous species. Although species' responses to changes in climate may vary, system-level phenology measurements at large spatial and temporal scales can inform how rapidly disruptions are affecting large assemblages of species. Our measures show that migration systems are exhibiting widespread phenological changes.

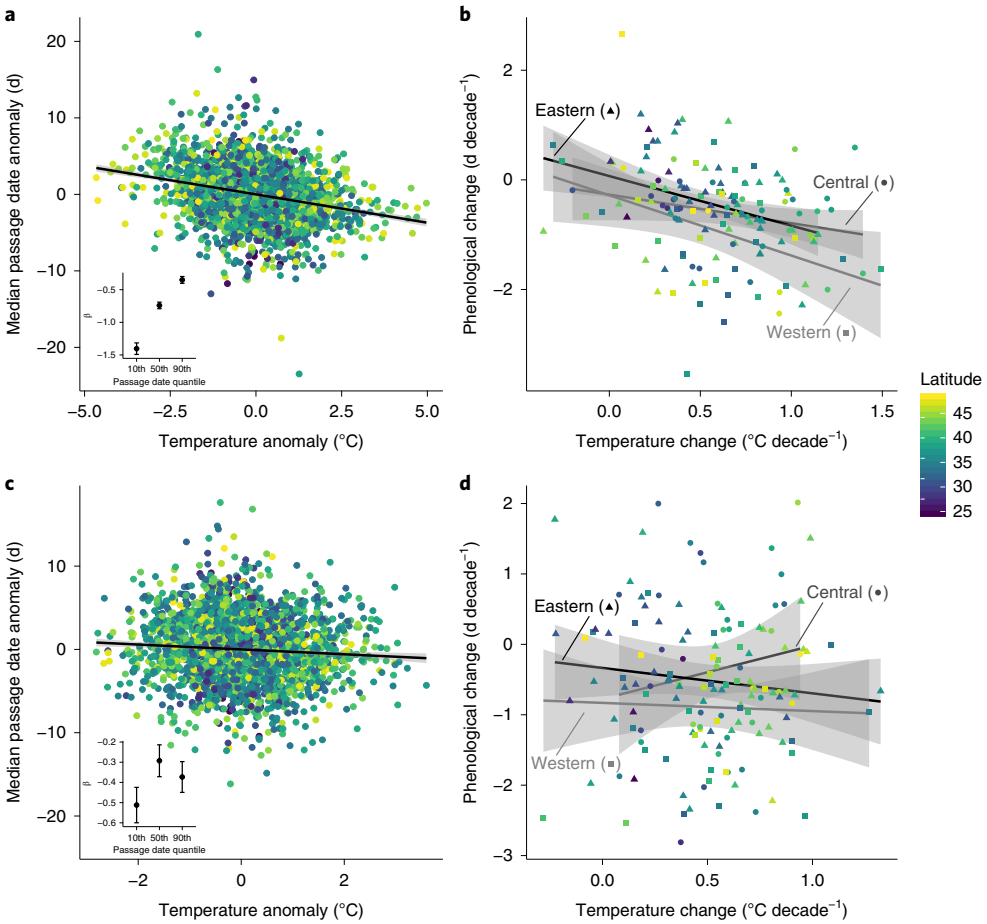

Fig. 4 | Anomaly and decadal change comparisons of migration phenology and annual temperature. a,**c**, Spring (**a**) and autumn (**c**) relationships between the median passage date anomaly and the temperature anomaly across all WSR stations. Insets: slope magnitude (β) and standard error of anomaly regressions across three quantiles of passage dates (10th, 50th, and 90th). **b**,**d**, Spring (**b**) and autumn (**d**) relationships between the decadal phenological change and temperature change across three North American flyways (western, central and eastern). Points are shaded according to the WSR station latitude, and the fitted lines and 95% confidence bands are from least-squares linear regression. For **b** and **c**, the point shapes are coded by flyway.

Online content

Any methods, additional references, Nature Research reporting summaries, source data, extended data, supplementary information, acknowledgements, peer review information; details of author contributions and competing interests; and statements of data and code availability are available at https://doi.org/10.1038/s41558-019-0648-9.

Received: 19 June 2019; Accepted: 31 October 2019;
Published online: 16 December 2019

References

1. Thackeray, S. J. et al. Phenological sensitivity to climate across taxa and trophic levels. *Nature* **535**, 241–245 (2016).
2. Parmesan, C. & Yohe, G. A globally coherent fingerprint of climate change impacts across natural systems. *Nature* **421**, 37–42 (2003).
3. Walther, G.-R. et al. Ecological responses to recent climate change. *Nature* **416**, 389–395 (2002).
4. Cohen, J. M., Lajeunesse, M. J. & Rohr, J. R. A global synthesis of animal phenological responses to climate change. *Nat. Clim. Change* **8**, 224–228 (2018).
5. Both, C. & Visser, M. E. Adjustment to climate change is constrained by arrival date in a long-distance migrant bird. *Nature* **411**, 296–298 (2001).
6. Parmesan, C. Ecological and evolutionary responses to recent climate change. *Annu. Rev. Ecol. Evol. Syst.* **37**, 637–669 (2006).
7. Cleland, E. E., Chuine, I., Menzel, A., Mooney, H. A. & Schwartz, M. D. Shifting plant phenology in response to global change. *Trends Ecol. Evol.* **22**, 357–365 (2007).
8. Saino, N. et al. Climate warming, ecological mismatch at arrival and population decline in migratory birds. *Proc. R. Soc. B* **278**, 835–842 (2011).
9. Jones, T. & Cresswell, W. The phenology mismatch hypothesis: are declines of migrant birds linked to uneven global climate change? *J. Anim. Ecol.* **79**, 98–108 (2010).
10. Hoffmann, A. A. & Sgrò, C. M. Climate change and evolutionary adaptation. *Nature* **470**, 479–485 (2011).
11. Chmura, H. E. et al. The mechanisms of phenology: the patterns and processes of phenological shifts. *Ecol. Monogr.* **89**, e01337 (2019).
12. Berthold, P. *Control of Bird Migration* (Chapman and Hall, 1996).
13. Both, C., Bouwhuis, S., Lessells, C. M. & Visser, M. E. Climate change and population declines in a long-distance migratory bird. *Nature* **441**, 81–83 (2006).
14. Butler, C. J. The disproportionate effect of global warming on the arrival dates of short-distance migratory birds in North America. *Ibis* **145**, 484–495 (2003).
15. Møller, A. P., Rubolini, D. & Lehikoinen, E. Populations of migratory bird species that did not show a phenological response to climate change are declining. *Proc. Natl Acad. Sci. USA* **105**, 16195–16200 (2008).
16. Kelly, J. F. & Horton, K. G. Toward a predictive macrosystems framework for migration ecology. *Glob. Ecol. Biogeogr.* **25**, 1159–1165 (2016).
17. Mayor, S. J. et al. Increasing phenological asynchrony between spring green-up and arrival of migratory birds. *Sci. Rep.* **7**, 1–10 (2017).
18. Jonzén, N. et al. Rapid advance of spring arrival dates in long-distance migratory birds. *Science* **312**, 1959–1961 (2006).
19. Balbontín, J. et al. Individual responses in spring arrival date to ecological conditions during winter and migration in a migratory bird. *J. Anim. Ecol.* **78**, 981–989 (2009).
20. Pettorelli, N. et al. Using the satellite-derived NDVI to assess ecological responses to environmental change. *Trends Ecol. Evol.* **20**, 503–510 (2005).

21. Horton, K. G. et al. Holding steady: little change in intensity or timing of bird migration over the Gulf of Mexico. *Glob. Change Biol.* **25**, 1106–1118 (2019).
22. Lin, T. et al. MISTNET: Measuring historical bird migration in the US using archived weather radar data and convolutional neural networks. *Methods Ecol. Evol.* **10**, 1908–1922 (2019).
23. La Sorte, F. A. et al. The role of atmospheric conditions in the seasonal dynamics of North American migration flyways. *J. Biogeogr.* **41**, 1685–1696 (2014).
24. Marra, P. P., Francis, C. M., Mulvihill, R. S. & Moore, F. R. The influence of climate on the timing and rate of spring bird migration. *Oecologia* **142**, 307–315 (2005).
25. Post, E., Steinman, B. A. & Mann, M. E. Acceleration of phenological advance and warming with latitude over the past century. *Sci. Rep.* **8**, 3927 (2018).
26. Bauer, S. et al. The grand challenges of migration ecology that radar aeroecology can help answer. *Ecography* **42**, 861–875 (2019).
27. Winger, B. M., Auteri, G. G., Pegan, T. M. & Weeks, B. C. A long winter for the Red Queen: rethinking the evolution of seasonal migration. *Biol. Rev.* **94**, 737–752 (2019).
28. Miller, R. A., Carlisle, J. D., Paprocki, N., Kaltenecker, G. S. & Heath, J. A. in *Phenological Synchrony and Bird Migration: Changing Climate and Seasonal Resources in North America* Vol. 47 (eds Wood, E. M. & Kellermann, J. L.) 177–191 (CRC, 2015).
29. Jarjour, C., Frei, B. & Elliott, K. H. Associations between sex, age and species-specific climate sensitivity in migration. *Anim. Migr.* **4**, 23–36 (2017).
30. Lameris, T. K. et al. Arctic geese tune migration to a warming climate but still suffer from a phenological mismatch. *Curr. Biol.* **28**, 2467–2473.e4 (2018).
31. Rakhimberdiev, E. et al. Fuelling conditions at staging sites can mitigate Arctic warming effects in a migratory bird. *Nat. Commun.* **9**, 1–10 (2018).
32. Carlisle, J. D. et al. Landbird migration in the American West: recent progress and future research directions. *Condor* **111**, 211–225 (2009).
33. Gill, J. A. et al. Why is timing of bird migration advancing when individuals are not? *Proc. R. Soc. B* **281**, 20132161 (2014).

Methods

Weather radar data acquisition. We quantified the intensity of avian migration to measure the phenology of migratory movements and computed the speed and direction to integrate traffic flows through the night from civil dusk to civil dawn (the Sun 6° below the horizon). We sampled nocturnal time periods because they capture the majority of migratory species that move through North America (~80% of migratory species)[34]. However, some taxonomic groups will not be represented in our analysis, including most soaring species (for example, those of Accipitridae, Cathartidae, Falconidae and Pelecanidae), aerial insectivores (for example, those of Hirundinidae) and some diurnally migrating passerines (for example, those of Fringillidae, Icteridae and Sturnidae). We used unfiltered (that is, level II) NEXRAD[35] WSR data from 143 stations from spring (1 March to 15 June) and autumn (1 August to 15 November) that encompassed spring 1995 through to spring 2018. We acquired radar data through the Amazon Web Service portal (https://s3.amazonaws.com/noaa-nexrad-level2/index.html), extracting data every 30 min from local sunset to sunrise. During the history of this sensor system, algorithmic changes occurred, which influenced how the data are processed. Although this is not a concern for phenological analyses, because we do not make comparisons of absolute magnitude across years, it is a concern when comparing absolute magnitudes. For this reason, we did not include changes in abundance because we sought to analyse the entirety of the NEXRAD archive. Rosenberg et al.[36] give ten-year radar-derived comparisons of abundance.

Clutter removal from weather radar data. Prior to constructing height profiles of migratory activity, we created binary masks separately for each calendar year and radar to remove stationary clutter (for example, buildings, wind turbines and terrain blockage) from the lowest elevational scan. We created masks by summing a minimum of 100 low-elevation scans (0.5°), starting on 1 January (16:00 UTC to 18:00 UTC) and continuing to 15 January. If 100 samples were unavailable by 15 January, we expanded the window of selection until the threshold was met. We classified any pixel above the 85th percentile of the summed reflectivity as clutter and masked it from our analyses[21].

Precipitation removal from WSR. To remove weather contamination, we trained a deep convolutional neural network (CNN) to segment regions of precipitation from the biology in WSR volume scans and set the reflectivity of any pixel to zero if it was classified as precipitation[22]. Precipitation and migratory movements tend to be mutually exclusive, with precipitation, especially heavy precipitation, halting the movement of migrants[37,38]. We trained the CNN using scans sampled at 30 min intervals for the first 3 h after the local sunset for all WSR stations in April, May, September and October 2014–2016 (239,128 scans in total). We assigned per-pixel training labels using polarimetric variables: if the correlation coefficient exceeded 0.95, reflectivity was classified as rain, otherwise it was classified as biological. The CNN used an FCN8 architecture[39] with a VGG-16 backbone[40] modified to the dimensions of the radar data, and was trained by back-propagation[41] and stochastic gradient descent[42]. The trained CNN classifies pixels using only legacy radar variables (for example, reflectivity, radial velocity and spectrum width), and may be run on any historical radar scan. We evaluated the performance on manually segmented scans that were both historically and geographically representative; the CNN retained 95.9% of all the biomass (summed reflectivity of the pixels classified as biology) with a false-positive rate of 1.3%.

Quantifying migration activity from filtered WSR data. From clutter- and precipitation-free data, we calculated the height profiles of migration intensity, speed and direction using the lowest elevation scans (0.5–4.5°), at distances between 5 and 37.5 km from the radar. We determined the migration intensity from reflectivity (η (cm^2 km^{-3})) and migrant flight direction (that is, track) and ground speed from the radial velocity from 100 to 3,000 m above ground level within 100 m altitudinal bins[43–46]. When necessary, we de-aliased the radial velocity measures using the WSRLIB package[47,48]. To limit the influence of migratory insects, we excluded altitudinal bins with velocity azimuth displays with a root mean squared error less than one, and we removed samples with a root mean squared error greater than ten to limit the poor fits[49,50]. We further restricted sampling nights to measures with seasonally appropriate flight directions, allowing only samples with a northward component in the spring and a southward component in the autumn (between 90 and 270°, depending on the season).

Quantifying traffic rate and peak migration date. To estimate the nightly passage of migrants at each WSR station, we first converted the reflectivity factor (decibel-transformed Z, dBZ) to reflectivity (dBη) following $\eta[\mathrm{dB}] = Z[\mathrm{dBZ}] + \beta$, where $\beta = 10\log_{10}(10^3\pi^5|K|^2/\lambda^4)$ (ref. [51]). We used an average WSR-88D wavelength (λ) of 10.7 cm and a dielectric factor ($|K|^2$) for liquid water of 0.93. This yielded $\beta = 13.37$. Converting Z to η resulted in units of cm^2 km^{-3}. To account for the flow of migrants over the sampling area, we multiplied cm^2 km^{-3} by the northward (or southward) component of the measured ground speed (km h^{-1}) and integrated through the night to account for the nightly passage using linear interpolation for the area under the curve, which resulting in units of cm^2 km^{-2}. We multiplied by the altitudinal resolution (0.1 km) of each altitudinal bin, which resulted in cm^2 km^{-1} per night.

We defined peak migration date as the date at which 50% of summed reflectivity was recorded for each radar station (Fig. 1). A single seasonal peak migration date was calculated for each WSR station for each year. Additionally, we calculated the dates at which 10 and 90% of the summed reflectivity were recorder to examine differential responses to temperature during early (10%), peak (50%) and late (90%) migration periods. We only included seasonal station time series in our analysis if more than 75% of the nights were sampled.

Quantifying change in date of peak migration. We examined phenological trends at two spatial levels,: (1) across the entire United States, to capture a continental-scale trend and (2) within three biogeographically distinct migration flyways (western, central and eastern[23]). Our flyway definitions were based on La Sorte et al.[23], which used a hierarchical cluster analysis to identify species with shared migration routes. The approach to delineate migration flyways was driven by eBird[52] probability-of-occurrence models from 93 migratory species.

To estimate the change in peak migration across the United States, we used a generalized additive mixed model (GAMM)[53]. We constructed the GAMM with the peak migration date as the response variable and used a tensor product smooth with an interaction between latitude and year, setting the smoothing parameters (k) to four and five for the respective terms. We used the station ID as a random effect to account for a unique station variation not captured by latitude. From the GAMM, we generated predictions of peak migration at four latitude bands (30, 35, 40 and 45°) and from 1996 to 2018 (spring) or to 2017 (autumn). We did not make predictions to 1995 because the number of representative stations in each flyway was limited (for example, <5 stations per flyway).

When conducting decadal change analyses, we required WSR station-specific estimates of phenological change. We obtained these from a linear model constructed with the WSR ID as a fixed effect and an interaction between the WSR ID and year. This yielded site-specific coefficients of phenological change for each WSR station. We applied a ridge-regression penalty (penalty = 0.0001) while fitting the model to control the variance of the station-specific slopes.

Quantifying change in the surface air temperature. To relate interannual variation in the peak migration with climate, we extracted data on the diurnal air temperatures (°C) at 2 m above ground from the NCEP North American Regional Reanalysis[54] for the same dates for which WSR data were analysed. We extracted diurnal temperature measures from the radar coverage area (37.5 km from the radar) and averaged the daily measures within each year, which resulted in a seasonal time series per WSR station. To quantify the seasonal change in surface temperature, we averaged the temperatures with season (spring or autumn) and used a ridge-regression linear model with WSR ID as a fixed effect and an interaction between WSR ID and year. This yielded site-specific coefficients of change for each WSR station. We used a penalty of 0.00001.

Temperature as a predictor of migration passage: annual anomaly and decadal change. We examined relationships between temperature and migration phenology at two levels: (1) annual anomaly and (2) decadal change. We calculated the anomalies as yearly deviations from station-specific means over the entire period for both passage dates and temperature. We used anomalies in this analysis to control for geography. A least-squares linear regression was used to relate the passage-date anomalies to the temperature anomalies, fit for early (10th), peak (50th) and late (90th) passage dates for each season. To quantify the dependence of phenological change (d decade^{-1}) on surface temperature change (°C decade^{-1}), we used a least-squares linear regression fit for each flyway for each season.

Data availability

The datasets generated during and/or analysed during the current study are available at https://doi.org/10.6084/m9.figshare.10062239.v1.

Code availability

Radar processing code and algorithms can be found at https://zenodo.org/record/3352264#.XXesby2ZPRY

References

34. Horton, K. G. et al. Bright lights in the big cities: migratory birds' exposure to artificial light. *Front. Ecol. Environ.* **17**, 209–214 (2019).
35. Crum, T. D., Alberty, R. L. & Burgess, D. W. Recording, archiving, and using WSR-88D data. *Bull. Am. Meteorol. Soc.* **74**, 645–653 (1993).
36. Rosenberg, K. V. et al. Decline of the North American avifauna. *Science* **366**, 120–124 (2019).
37. Richardson, W. J. Timing and amount of bird migration in relation to weather: a review. *Oikos* **30**, 224–272 (1978).
38. Richardson, W. J. in *Bird Migration* (ed. Gwinner, E.) 78–101 (Springer, 1990).
39. Long, J., Darrell, T. & Shelhamer, E. Fully convolutional networks for semantic segmentation. In *2015 IEEE Conference on Computer Vision and Pattern Recognition (CVPR)* 3431–3440 (IEEE, 2015).
40. Simonyan, K. & Zisserman, A. Very deep convolutional networks for large-scale image recognition. Preprint at https://arxiv.org/abs/1409.1556 (2015).

41. Rumelhart, D. E., Hinton, G. E. & Williams, R. J. Learning representations by back-propagating errors. *Nature* **323**, 533–536 (1986).
42. Goodfellow, I., Bengio, Y. & Courville, A. *Deep Learning* (MIT, 2016).
43. Farnsworth, A. et al. A characterization of autumn nocturnal migration detected by weather surveillance radars in the northeastern US. *Ecol. Appl.* **26**, 752–770 (2016).
44. Browning, K. A. & Wexler, R. The determination of kinematic properties of a wind field using Doppler radar. *J. Appl. Meteor.* **7**, 105–113 (1968).
45. Buler, J. J. & Diehl, R. H. Quantifying bird density during migratory stopover using weather surveillance radar. *IEEE Trans. Geosci. Remote Sens.* **47**, 2741–2751 (2009).
46. Horton, K. G., Van Doren, B. M., Stepanian, P. M., Farnsworth, A. & Kelly, J. F. Where in the air? Aerial habitat use of nocturnally migrating birds. *Biol. Lett.* **12**, 20160591 (2016).
47. Sheldon, D. et al. Approximate Bayesian inference for reconstructing velocities of migrating birds from weather radar. In *Proceedings of the Twenty-Seventh AAAI Conference on Artificial Intelligence* 1334–1340 (AAAI, 2013).
48. Sheldon, D. WSRLIB: MATLAB Toolbox for Weather Surveillance Radar (Bitbucket, 2015); https://bitbucket.org/dsheldon/wsrlib
49. Dokter, A. M. et al. Bird migration flight altitudes studied by a network of operational weather radars. *J. R. Soc. Interface* **8**, 30–43 (2011).
50. Horton, K. G., Van Doren, B. M., Stepanian, P. M., Farnsworth, A. & Kelly, J. F. Seasonal differences in landbird migration strategies. *Auk* **133**, 761–769 (2016).
51. Chilson, P. B. et al. Estimating animal densities in the aerosphere using weather radar: to *Z* or not to *Z*? *Ecosphere* **3**, art72 (2012).
52. Sullivan, B. L. et al. The eBird enterprise: an integrated approach to development and application of citizen science. *Biol. Conserv.* **169**, 31–40 (2014).
53. Wood, S. mgcv: mixed GAM computation vehicle with GCV/AIC/REML smoothness estimation. R package version 1.8-28 (2015).
54. Mesinger, F. et al. North American regional reanalysis. *Bull. Am. Meteorol. Soc.* **87**, 343–360 (2006).

Acknowledgements

NSF Advances in Biological Informatics (ABI-1661259), Division of Information and Intelligent Systems (IIS-1633206) and Integrative and Collaborative Education and Research (1927743) programmes, as well as a Leon Levy Foundation and an Edward W. Rose Postdoctoral Fellowship supported this research.

Author contributions

All the authors worked to conceive and design this study. K.G.H., F.A.L., D.S. and A.F. drafted the manuscript. T.-Y.L., K.W., G.B., S.M., K.G.H. and D.S. designed the radar algorithms, and processed and summarized the radar data. K.G.H. generated the figures and D.S., W.M.H. and K.G.H. designed the analyses. All the authors provided editorial advice, approved the final version of this manuscript and are in agreement to be accountable for all aspects of the work.

Competing interests

The authors declare no competing interests.

Additional information

Correspondence and requests for materials should be addressed to K.G.H.